Graphene nanoplatelets for electrically conductive 3YTZP composites densified by pressureless sintering

Cristina López-Pernía [a,*], Ángela Gallardo-López[a], Ana Morales-Rodríguez[a], Rosalía Poyato [b]

a. Dpto. de Física de la Materia Condensada. ICMS, CSIC-Universidad de Sevilla. Apdo. 1065. 41080 Sevilla. Spain

b. Inst. Ciencia de Materiales de Sevilla, ICMS, CSIC-Universidad de Sevilla. Américo Vespucio 49. 41092 Sevilla. Spain.

*Corresponding author. E-mail address: cristinalopez@us.es

Abstract

3 mol% yttria tetragonal zirconia polycrystalline (3YTZP) ceramic composites with 2.5, 5 and 10 vol% graphene nanoplatelets (GNP) were pressureless sintered in argon atmosphere between 1350 and 1450 ºC. The effects of the GNP content and the sintering temperature on the densification, microstructure and electrical properties of the composites were investigated. An isotropic distribution of GNP surrounding ceramic regions was exhibited regardless the GNP content and sintering temperature used. Electrical conductivity values comparable to the ones of fully dense composites prepared by more complex techniques were obtained, even though full densification was not achieved. While the composite with 5 vol% GNP exhibited electrical anisotropy with a semiconductor-type behaviour, the composite with 10 vol% GNP showed an electrically isotropic metallic-type behaviour.

Keywords: graphene nanoplatelet, zirconia, pressureless sintering, electrical properties,

1. Introduction

Ceramics are widely known for their hardness and chemical stability but also for their brittleness and thermal and electrical insulation behaviour. Graphene-based nanomaterials (GBN) exhibit exceptional properties and functionalities comparable to those of monolayer graphene [1] while presenting a competitive cost. Therefore, they appear as attractive candidates as fillers in engineering advanced ceramic materials with the idea of taking advantage of the properties of GBN to enhance the mechanical, thermal and electrical properties of ceramic. Concerning this last point, it has been reported that it is possible to tune the electrical properties of ceramic composites by adding the appropriate amount of GBN. Turning ceramics into suitably electrically conductive materials (σ > 0.3-1 S/m) opens the door to manufacturing techniques such as electro-discharge machining (EDM) [2]. In the last decade, many researchers have studied the incorporation of GBN into a wide variety of ceramic matrices such as Si_3N_4, SiC, Al_2O_3, ZrO_2 or B_4C [3–5]. Among the advanced ceramics, 3 mol% yttria tetragonal zirconia polycrystalline (3YTZP) is a very interesting ceramic material since it presents excellent mechanical properties, particularly its high fracture toughness, good wear resistance and chemical stability [6]. However, the knowledge about GBN/3YTZP composites and their electrical behaviour is still very limited.

The consolidation of the GBN/ceramic composites is typically carried out by sintering techniques which involve uniaxial pressure, such as spark plasma sintering (SPS) or hot pressing (HP). However, these techniques require expensive equipment and produce highly anisotropic materials [7–11]. Pressureless sintering (PLS) is a cheaper and attractive technique which allows fabrication of materials with larger dimensions and complex shapes. This conventional method presents a high potential for scaling-up the fabrication of advanced ceramic composites to an industrial level. Nevertheless, to our knowledge, the studies about fabrication of GBN/ceramic composites sintered by conventional methods are scarce. Taking into account the possible applications of these materials, studying the electrical properties of these PLSed composites becomes a really attractive topic.

In this work, the sintering behavior of GNP/3YTZP composites with 2.5 to 10 vol% filler loading using the PLS technique, and the effect of the GNP incorporation on the

densification, microstructure and electrical conductivity of the composites have been assessed.

2. Experimental procedure

2.1 Composite powder processing and sintering

The as-received 3YTZP powder (40 nm particle size, Tosoh Corporation, Tokyo, Japan) was annealed at 850°C for 30 min in air. The composite powders were prepared using commercially available GNP with ≤ 5 μm planar diameter and 10-20 nm thickness (N006-P, Angstron Materials, Dayton, Ohio, USA) by wet powder processing in isopropanol using ultrasonic agitation. The full procedure is described in [8].

The green bodies were preformed as disc samples (20 mm diameter, 3 g weight) by uniaxial pressing at 90 MPa followed by cold isostatic pressing at 200 MPa. The green bodies were pressureless sintered under Ar flow at three different temperatures (1350, 1400 and 1450 °C), using a heating ramp of 5 ºC/min and 2 hour holding time. With the aim of evaluating the effect of the GNP incorporation in the ceramic matrix, monolithic 3YTZP ceramics were also prepared using similar sintering conditions.

2.2. Characterization of the sintered specimens

The bulk density of the sintered samples was determined using the Arquimedes' method in distilled water. The theoretical density of the composites was determined by the rule of mixtures taking the density of the 3YTZP and the GNP as 6.05 g/cm^3 and 2.2 g/cm^3, respectively.

2.2.1. Microstructural characterization

The crystallographic phases of the sintered pellets were analyzed by X-Ray diffraction (XRD) at Centro de Investigación, Tecnología e Innovacion de la Universidad de Sevilla (CITIUS).

Raman spectroscopy was used in order to account for any structural damage of the GNP during the powder processing or sintering. The spectra were recorded using a dispersive microscope (Horiba Jobin Yvon LabRam HR800, Kyoto, Japan). Six to eight spectra were obtained from the composite powders prior to sintering and also from the fracture surfaces of the PLSed composites.

The analysis of the GNP distribution in the 3YTZP matrix was carried out by scanning electron microscopy (SEM). The fracture surfaces of the sintered samples were inspected by high resolution scanning electron microscopy (HRSEM, Hitachi S5200, CITIUS). Cross-section (c.s.) surfaces, polished with diamond paste up to 1 μm, were observed by conventional SEM (Zeiss Evo, CITIUS) using back-scattered electrons (BSE) for imaging.

2.2.2. Electrical conductivity

The electrical characterization was carried out by impedance spectroscopy using an Agilent 4294A analyzer. In order to collect data in a temperature range from room temperature to 450 ºC, the samples were placed inside an alumina tubular furnace. The electrical measurements were carried out in Ar atmosphere to avoid the oxidation of the composites and the subsequent degradation of the GNP during the process. The electrodes were prepared by applying colloidal silver paste on both sides of the samples and heating up to 600 ºC for 30 min under Ar flow. The electrical conductivity was acquired in the directions parallel ($\sigma_{\parallel}$) and perpendicular ($\sigma_{\perp}$) to the uniaxial pressing axis to account for any degree of electrical anisotropy. To this end, the electrodes were set on the in-plane and cross-section surfaces of the samples, respectively.

3. Results and discussion

A detrimental effect of the GNP addition on the relative density of the samples regardless the sintering temperature is observed (Figure 1). The highest relative densities (up to 98.9 %) are obtained in the monolithic zirconia for all the sintering temperatures, although these values are slightly lower than the reported ones in other works, where densities higher than 99% are obtained [6,12]. As the GNP content increases, the relative density of the composites decreases, being this effect especially remarkable for the composites with 10 vol% GNP. The decrease in densification is in good agreement with previous investigations, in which the direct influence of the GNP content on the density of ceramic composites prepared by PLS is clearly stated [6,13,14]. Yang et al. [14] reported that, although a small fraction of graphene filler facilitates the densification process of GNP/Si_3N_4 composites, an excessive graphene content could decrease the relative density of the material due to the pores formed between GNP and ceramic matrix. In this sense, Li et al. [13] also reported a monotonical decrease of the relative density from ~99 % to ~96 % when increasing the graphene content up to 5 wt% in SiC composites and Ramesh

et al. [6] obtained zirconia composites with relative densities also decreasing from ~98 to ~96 % by using small amounts of graphene oxide up to 1 wt%.

3.1 Microstructure

The XRD analysis conducted on the monolithic 3YTZP ceramic and the GNP/3YTZP composites indicated the presence of reduced tetragonal zirconia ($ZrO_{1.95}$) (JCPDS 081-1544) as the main phase for all sintering temperatures (supplementary figure S1). For the highest GNP content (10 vol%), there is a detectable carbide phase (ZrC, JCPDS 065-0973) indicative of a reaction between the 3YTZP matrix and the GNP during sintering.

The Raman spectra of all composites displayed the D-band at ~1350 cm^{-1}, the G-band at ~1585 cm^{-1} and the 2D-band at ~2700 cm^{-1} (supplementary figure S2), which are the characteristic peaks for the GNP [8]. The D-band is usually described as the disorder band for graphitic materials, so high values of I_D/I_G are associated to disorder or defects in the material [15]. Figure 2 shows the I_D/I_G ratios as a function of the sintering temperature and the GNP content for all the prepared composites. For a sintering temperature of 1350 ºC, low values of I_D/I_G (~ 0.12) are obtained without significant changes in the I_D/I_G ratio as the content of GNP increases. These values are similar to the recently reported ones for 3YTZP composites with 2.5, 5 and 10 vol% GNP consolidated by SPS [8]. The I_D/I_G values for the composites sintered at 1400 ºC are slightly higher than the previous ones and they are also similar to each other for the different GNP contents. These results indicate the preservation of the GNP during sintering at 1350 and 1400 ºC. However, when the sintering temperature increases up to 1450 ºC, the I_D/I_G values significantly increase, especially for the composites with 2.5 and 5 vol% GNP. This suggests that the GNP could have been damaged due to long time exposure (2 hours) at the highest temperature used for sintering in the present work..

In order to observe the distribution of the GNP in the matrix, the c.s. polished surfaces of the composites sintered at 1350 ºC have been analyzed by BSE (figure 3). Due to the average atomic number difference between the two phases of the composite, BSE can be used to detect contrast between the different elemental compositions in the sample. The light phase corresponds to the 3YTZP matrix and the dark phase to the GNP. A nearly homogeneous GNP distribution throughout the ceramic matrix can be seen in figure 3. The GNP tend to form interconnected groups surrounding wide circular ceramic areas (40 µm diameter). These GNP-free areas are a consequence of the formation of ceramic

powder clusters before the sintering process. Therefore, processing efforts shall be carried out to avoid their formation in future works. Despite using uniaxial pressure during the green body preparation, no preferential GNP alignment in the c.s. surfaces is observed. As it can be seen in figure 3, the GNP present very different orientations, so that they are able to surround the ceramic regions. As the GNP content increases, the contouring of the ceramic areas is more remarkable. This isotropic distribution of the GNP is notably different than the reported one for composites prepared by SPS, where the GNP ab-plane is preferentially aligned perpendicular to the SPS pressing axis [8,16].

The HRSEM images of the fracture surfaces (figure 4) allow having an insight about the size and shape of the graphene fillers. It is possible to see large overlapping interconnected groups of GNP with different shapes. These features contribute to the formation of voids between the overlapping GNP and at the ceramic-GNP interfaces. Although pores are not clearly found in the ceramic matrix, these voids at the interfaces and the crumpling of rolled-up GNP may contribute to the porosity and, hence, to the decrease in relative density of the composites in agreement with [14].

3.2 Electrical conductivity

The room temperature electrical conductivity acquired in the two electrode configurations of the GNP/3YTZP composites sintered at 1350 ºC and 1400 ºC is shown in table 1. Monolithic 3YTZP is known to be an electrically isolating material at room temperature. However, reduced tetragonal zirconia has been reported to present some electrical conductivity depending on its reduction level [17]. In this work, the composites with 2.5 vol% GNP show low conductivity values which can be associated to the reduced tetragonal zirconia electrical behaviour. The addition of 5 vol% GNP promotes a remarkable increase in the conductivity, indicating that the GNP network is percolated. Regardless of the used sintering temperature, the electrical percolation threshold is estimated to be situated between 2.5 and 5 vol% GNP which is in good agreement with previously published works of SPSed composites. Fan et al. reported a percolation threshold around 3 vol% graphene sheets in alumina composites [18] while, regarding zirconia matrices, percolation thresholds around 2.5 vol% have been obtained for GNP [8] and reduced graphene oxide [19] fillers.

The highest electrical conductivity measured in these composites is 177 ± 7 S/m for the one with 10 vol% GNP sintered at 1350 ºC. Figure 5 shows an overview of the electrical

conductivity values measured in different works on composites sintered by SPS and PLS. Higher values have been reported by Markandan et al. for PLSed zirconia composites with a lower amount of GNP filler (280 S/m for 5.5 vol%) [20] in comparison with our results. However, our conductivity value is still much higher than the obtained one by Li et al. (1.82 S/m) in PLSed SiC composites with a higher graphene content (13.75 vol%) [13]. The electrical characterization of pressureless sintered zirconia composites is still very limited and only a few studies have been carried out in this sense. In SPSed composites, Shin et al. [19] achieved an electrical conductivity of 12000 S/m with 4.1 vol% reduced graphene oxide and Kwon et al. [21] obtained 98 S/m with 8.25 vol% graphene flakes. The significant differences in the reported values of electrical conductivity may be attributed to the distinct types of GBN used and their different aspect ratios [3,11]. In a recent study, a comparison between the electrical behaviour of 3YTZP composites with GNP and with few-layered graphene (FLG) has been reported [11]. For the same GBN content, the composites with FLG have higher electrical conductivity than the ones with GNP. When using the SPS technique instead of PLS, only slightly higher values of electrical conductivity (239 S/m) are obtained for composites with the same amount of GNP (10 vol%) and the same powder processing routine [11].

Independently of the GNP content and sintering temperature, $\sigma_{\perp}$ is higher than $\sigma_{\parallel}$ in all cases revealing a slight electrical anisotropy in the PLSed composites of our study (table 1). This indicates a slight preferential orientation of the GNP that has not been perceived by the microstructural observations. The slight conductivity variations with sintering temperature could be associated to the changes in densification.

In the composites with 5 vol% GNP, the values of electrical anisotropy are similar to the obtained ones in SPSed samples [16]. However, the anisotropy factor decreases remarkably for 10 vol% GNP. In this case, the results are very different from the reported ones in SPSed samples [7,11] where the GNP network is better percolated in the perpendicular configuration due to the preferential alignment of the GNP perpendicularly to the SPS pressing axis.

The electrical conductivity data acquired as a function of temperature for the composites with 5 and 10 vol% GNP sintered at 1350 ºC (supplementary figure S3) have been plotted according to a model that describes a thermally-assisted conduction through disordered regions (two-dimensional variable-range hopping, 2D-VRH, model). This model has

been previously applied to describe the electrical transport in graphene ceramic composites [16,22,23]. In the composite with 5 vol% GNP, a semiconductor-type behaviour is observed, i.e. as the temperature increases, the electrical conductivity increases ($(d\sigma/dT) > 0$). This behaviour can be properly described by the 2D-VRH mechanism of the charge carriers as the interconnections between the GNP are not complete and the isolating ceramic regions act as defects (figure 3b). Therefore, the conduction mechanism that takes place in this composite is based on the hopping of the charge carriers between the GNP, which is favored as the temperature increases. This behaviour is in good agreement with previous works of SPSed 3YTZP composites with 5 vol% GNP [16]. On the other hand, a negative $d\sigma/dT$ slope is observed in the plotted $\sigma_{\perp}$ data for the composite with 10 vol% GNP. In this case, as the temperature increases, the $\sigma_{\perp}$ decreases, so a metallic-type behaviour is taking place. Thus, the 2D-VRH model does not describe properly this composite. The behaviour in this case is the consequence of the charge transport along the main ab-plane of the nanoplatelets, since GNP are mostly free of defects and they are interconnected forming a well percolated network, as it was observed in the microstructure images (figure 3c). A similar behaviour in $\sigma_{\perp}$ was also previously reported in SPSed 3YTZP composites with 10 vol% GNP [16]. The value of $\sigma_{\parallel}$ for the composite with 10 vol% GNP remains stable with temperature in contrast with SPSed ones [16], whose behaviour in the parallel configuration was semiconductor-type. In those composites there were ceramic areas to be overcome by the carriers, but in our PLSed composites, the GNP surround those islands, meaning that there are not isolating regions to hop. Therefore, in this case, a transition to a metallic-type behaviour is taking place.

4 Conclusions

In this work, 3YTZP composites with 2.5, 5 and 10 vol% GNP have been consolidated by conventional pressureless sintering. Electrical conductivity values comparable to that of SPSed fully dense composites have been obtained, despite the decrease in the relative density of the composites due to the GNP addition. While the composite with 5 vol% GNP exhibits electrical anisotropy, the composite with 10 vol% GNP shows a nearly isotropic electrical behaviour for both studied configurations. A metallic-type behaviour is exhibited by the composite with 10 vol% GNP and a semiconductor-type one for the composite with 5 vol% GNP. The observed different electrical behaviours with

temperature are strongly correlated with the GNP distribution. Pressureless sintering has been shown to be a convenient technique for producing conducting zirconia composites with graphene nanoplatelets.

Acknowledgments

This work was supported by the Spanish Ministerio de Economía y Competitividad, under project MAT2015-67889-P, cofunded by European funding (ERDF).

References

[1] A. Bianco, H.-M. Cheng, T. Enoki, Y. Gogotsi, R.H. Hurt, N. Koratkar, T. Kyotani, M. Monthioux, C.R. Park, J.M.D. Tascon, J. Zhang, All in the graphene family – A recommended nomenclature for two-dimensional carbon materials, Carbon N. Y. 65 (2013) 1–6. doi:10.1016/j.carbon.2013.08.038.

[2] J.-W. Sung, K.-H. Kim, M.-C. Kang, Effects of graphene nanoplatelet contents on material and machining properties of GNP-dispersed Al_2O_3 ceramics for micro-electric discharge machining, Int. J. Precis. Eng. Manuf. Technol. 3 (2016) 247–252. doi:10.1007/s40684-016-0032-4.

[3] P. Miranzo, M. Belmonte, M.I. Osendi, From bulk to cellular structures: A review on ceramic/graphene filler composites, J. Eur. Ceram. Soc. 37 (2017) 3649–3672. doi:10.1016/j.jeurceramsoc.2017.03.016.

[4] V. Dhand, K.Y. Rhee, H. Ju Kim, D. Ho Jung, A comprehensive review of graphene nanocomposites: Research status and trends, J. Nanomater. 2013 (2013) 1–14. doi:10.1155/2013/763953.

[5] H. Porwal, P. Tatarko, S. Grasso, J. Khaliq, I. Dlouhý, M.J. Reece, Graphene reinforced alumina nano-composites, Carbon N. Y. 64 (2013) 359–369. doi:10.1016/j.carbon.2013.07.086.

[6] S. Ramesh, M.M. Khan, H.C. Alexander Chee, Y.H. Wong, P. Ganesan, M.G. Kutty, U. Sutharsini, W.J.K. Chew, A. Niakan, Sintering behaviour and properties of graphene oxide-doped Y-TZP ceramics, Ceram. Int. 42 (2016) 17620–17625. doi:10.1016/j.ceramint.2016.08.077.

[7] Á. Gallardo-López, C. López-Pernía, C. Muñoz-Ferreiro, C. González-Orellana, A. Morales-Rodríguez, R. Poyato, Spark plasma sintered zirconia ceramic composites with graphene-based nanostructures, Ceramics. 1 (2018) 153–164. doi:10.3390/ceramics1010014.

[8] A. Gallardo-López, I. Márquez-Abril, A. Morales-Rodríguez, A. Muñoz, R. Poyato, Dense graphene nanoplatelet/yttria tetragonal zirconia composites: Processing, hardness and electrical conductivity, Ceram. Int. 43 (2017) 11743–11752. doi:10.1016/j.ceramint.2017.06.007.

[9] O. Hanzel, R. Sedlák, J. Sedláček, V. Bizovská, R. Bystrický, V. Girman, A. Kovalčíková, J. Dusza, P. Šajgalík, Anisotropy of functional properties of SiC composites with GNP, GO and in-situ formed graphene, J. Eur. Ceram. Soc. 37

(2017) 3731–3739. doi:10.1016/j.jeurceramsoc.2017.03.060.

[10] O. Tapasztó, L. Tapasztó, H. Lemmel, V. Puchy, J. Dusza, C. Balázsi, K. Balázsi, High orientation degree of graphene nanoplatelets in silicon nitride composites prepared by spark plasma sintering, Ceram. Int. 42 (2016) 1002–1006. doi:10.1016/j.ceramint.2015.09.009.

[11] C. Muñoz-Ferreiro, A. Morales-Rodríguez, T.C. Rojas, E. Jiménez-Piqué, C. López-Pernía, R. Poyato, A. Gallardo-López, Microstructure, interfaces and properties of 3YTZP ceramic composites with 10 and 20 vol% different graphene-based nanostructures as fillers, J. Alloys Compd. 777 (2019) 213–224. doi:10.1016/j.jallcom.2018.10.336.

[12] M. Trunec, Effect of grain size on mechanical properties of 3Y-TZP ceramics, Ceram. - Silikaty. 52 (2008) 165–171. doi:10.1016/0956-7151(94)00253-E.

[13] Q. Li, Y. Zhang, H. Gong, H. Sun, T. Li, X. Guo, S. Ai, Effects of graphene on the thermal conductivity of pressureless-sintered SiC ceramics, Ceram. Int. 41 (2015) 13547–13552. doi:10.1016/j.ceramint.2015.07.149.

[14] Y. Yang, B. Li, C. Zhang, S. Wang, K. Liu, B. Yang, Fabrication and properties of graphene reinforced silicon nitride composite materials, Mater. Sci. Eng. A. 644 (2015) 90–95. doi:10.1016/j.msea.2015.07.062.

[15] I. Childres, L. Jauregui, W. Park, H. Cao, Y. Chen, Raman spectroscopy of graphene and related materials, in: New Dev. Phot. Mater. Res., 2013: pp. 1–20.

[16] R. Poyato, J. Osuna, A. Morales-Rodríguez, Á. Gallardo-López, Electrical conduction mechanisms in graphene nanoplatelet/yttria tetragonal zirconia composites, Ceram. Int. 44 (2018) 14610–14616. doi:10.1016/j.ceramint.2018.05.082.

[17] R. Poyato, J. Macías-Delgado, A. García-Valenzuela, R.L. González-Romero, A. Muñoz, A. Domínguez-Rodríguez, Electrical properties of reduced 3YTZP ceramics consolidated by spark plasma sintering, Ceram. Int. 42 (2016) 6713–6719. doi:10.1016/j.ceramint.2016.01.040.

[18] Y. Fan, L. Wang, J. Li, J. Li, S. Sun, F. Chen, L. Chen, W. Jiang, Preparation and electrical properties of graphene nanosheet/Al_2O_3 composites, Carbon N. Y. 48 (2010) 1743–1749. doi:10.1016/j.carbon.2010.01.017.

[19] J.-H. Shin, S.-H. Hong, Fabrication and properties of reduced graphene oxide reinforced yttria-stabilized zirconia composite ceramics, J. Eur. Ceram. Soc. 34 (2014) 1297–1302. doi:10.1016/j.jeurceramsoc.2013.11.034.

[20] K. Markandan, J.K. Chin, M.T.T. Tan, Enhancing electroconductivity of ytria-stabilised zirconia ceramic using graphene platlets, Key Eng. Mater. 690 (2016) 1–5. doi:10.4028/www.scientific.net/KEM.690.1.

[21] S.M. Kwon, S.J. Lee, I.J. Shon, Enhanced properties of nanostructured ZrO_2-graphene composites rapidly sintered via high-frequency induction heating, Ceram. Int. 41 (2014) 835–842. doi:10.1016/j.ceramint.2014.08.042.

[22] C. Ramirez, F.M. Figueiredo, P. Miranzo, P. Poza, M.I. Osendi, M. Isabel Osendi, Graphene nanoplatelet/silicon nitride composites with high electrical conductivity, Carbon N. Y. 50 (2012) 3607–3615. doi:10.1016/j.carbon.2012.03.031.

[23] B. Román-Manso, E. Domingues, F.M. Figueiredo, M. Belmonte, P. Miranzo, Enhanced electrical conductivity of silicon carbide ceramics by addition of graphene nanoplatelets, J. Eur. Ceram. Soc. 35 (2015) 2723–2731. doi:10.1016/j.jeurceramsoc.2015.03.044.

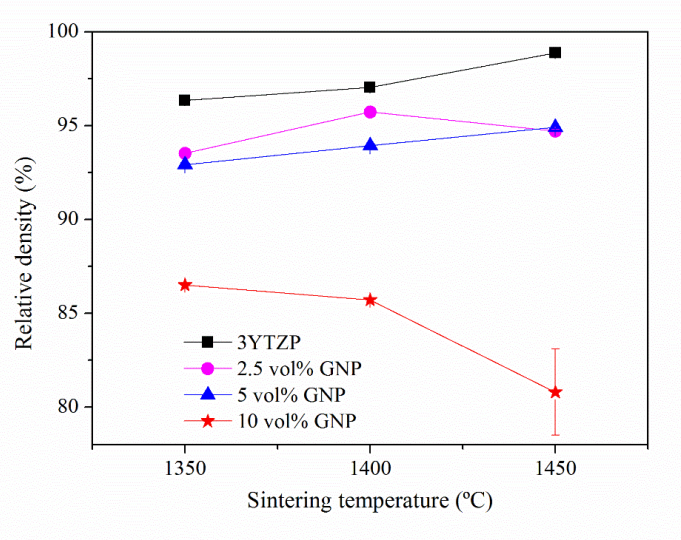
100
95
90
85
80
Relative density (%)
1350
1400
1450
Sintering temperature (ºC)
3YTZP
2.5 vol% GNP
5 vol% GNP
10 vol% GNP

Figure 1

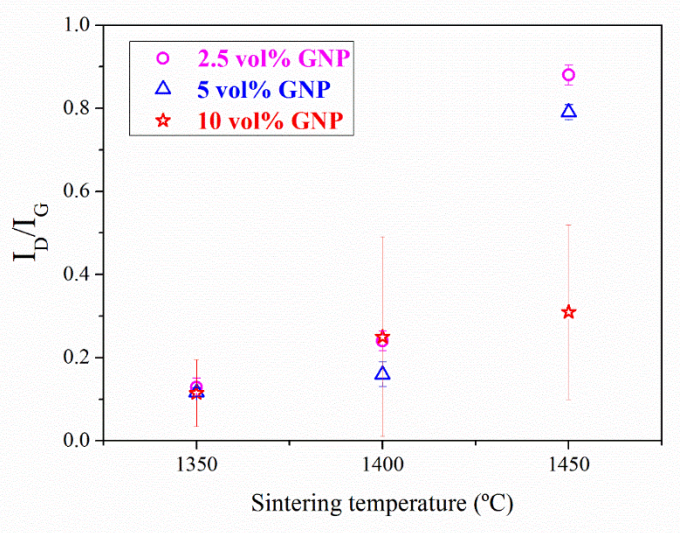
2.5 vol% GNP
5 vol% GNP
10 vol% GNP
I_D/I_G
1.0
0.8
0.6
0.4
0.2
0.0
1350
1400
1450
Sintering temperature (°C)

Figure 2

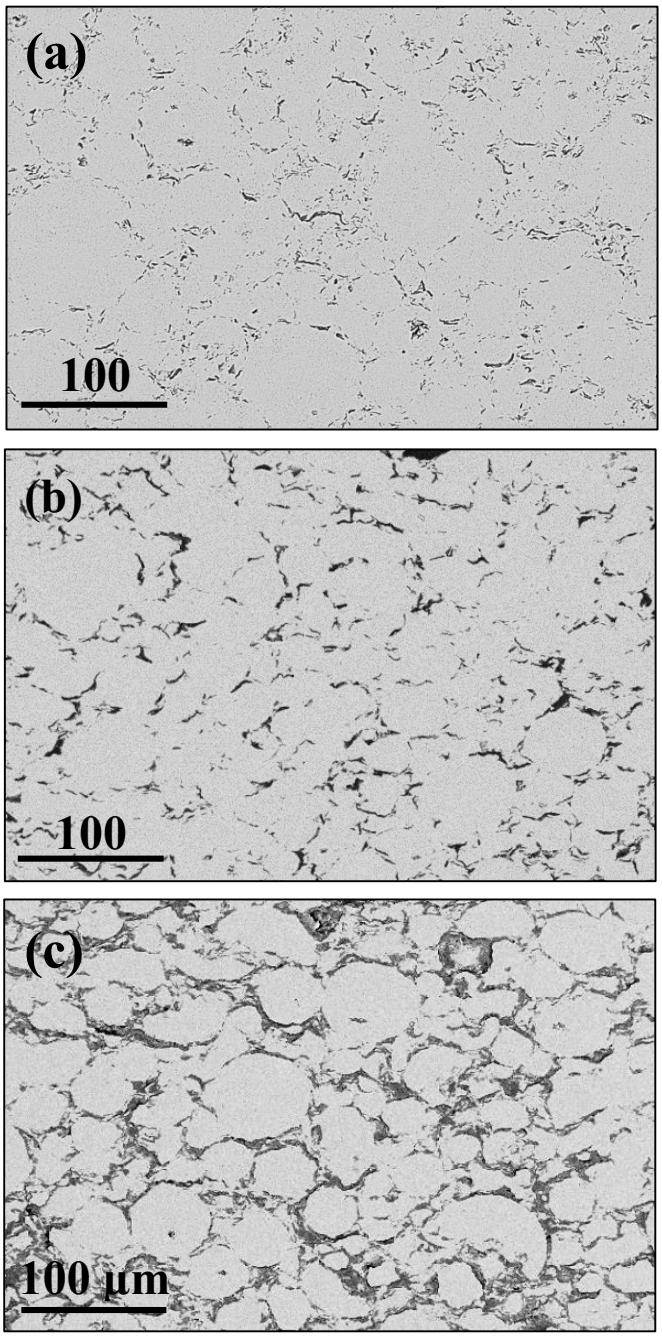

Figure 3

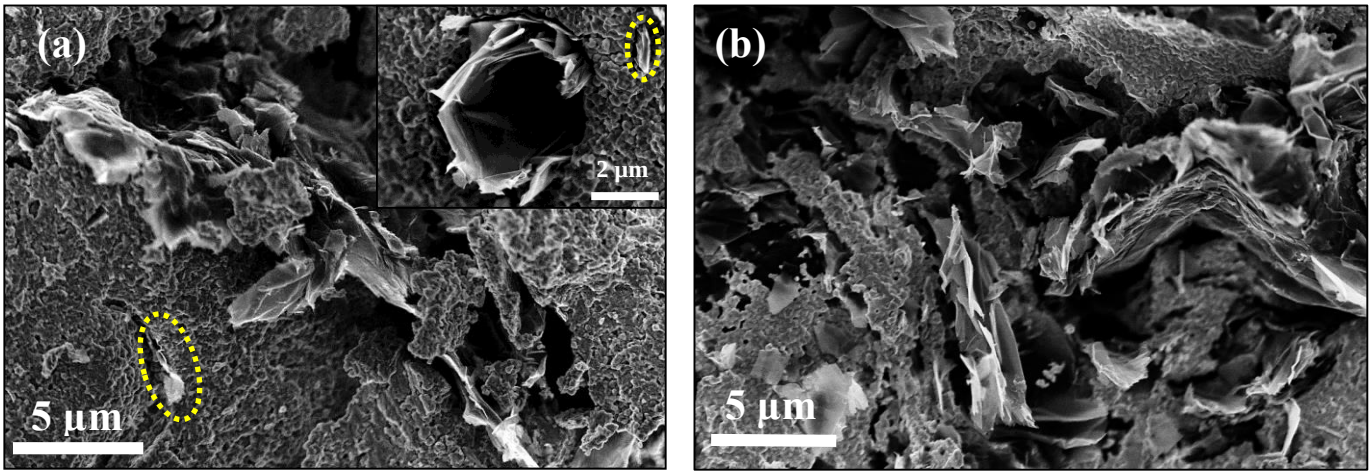

Figure 4

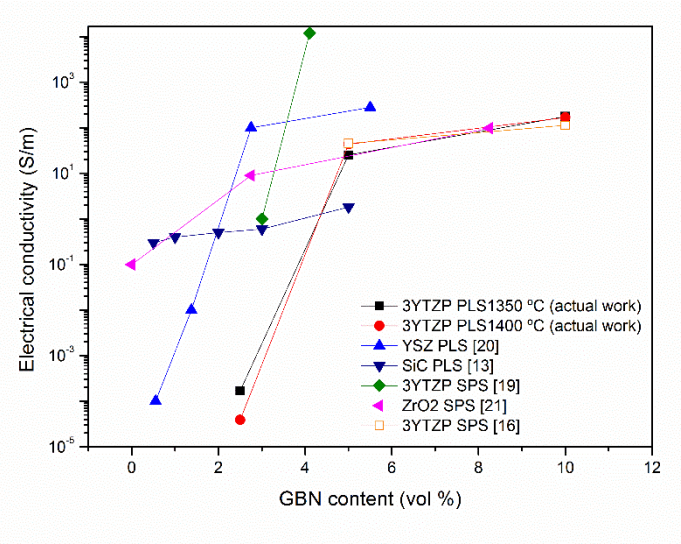
Electrical conductivity (S/m)
GBN content (vol %)
3YTZP PLS1350 ºC (actual work)
3YTZP PLS1400 ºC (actual work)
YSZ PLS [20]
SiC PLS [13]
3YTZP SPS [19]
ZrO2 SPS [21]
3YTZP SPS [16]

Figure 5

SUPPLEMENTARY INFORMATION

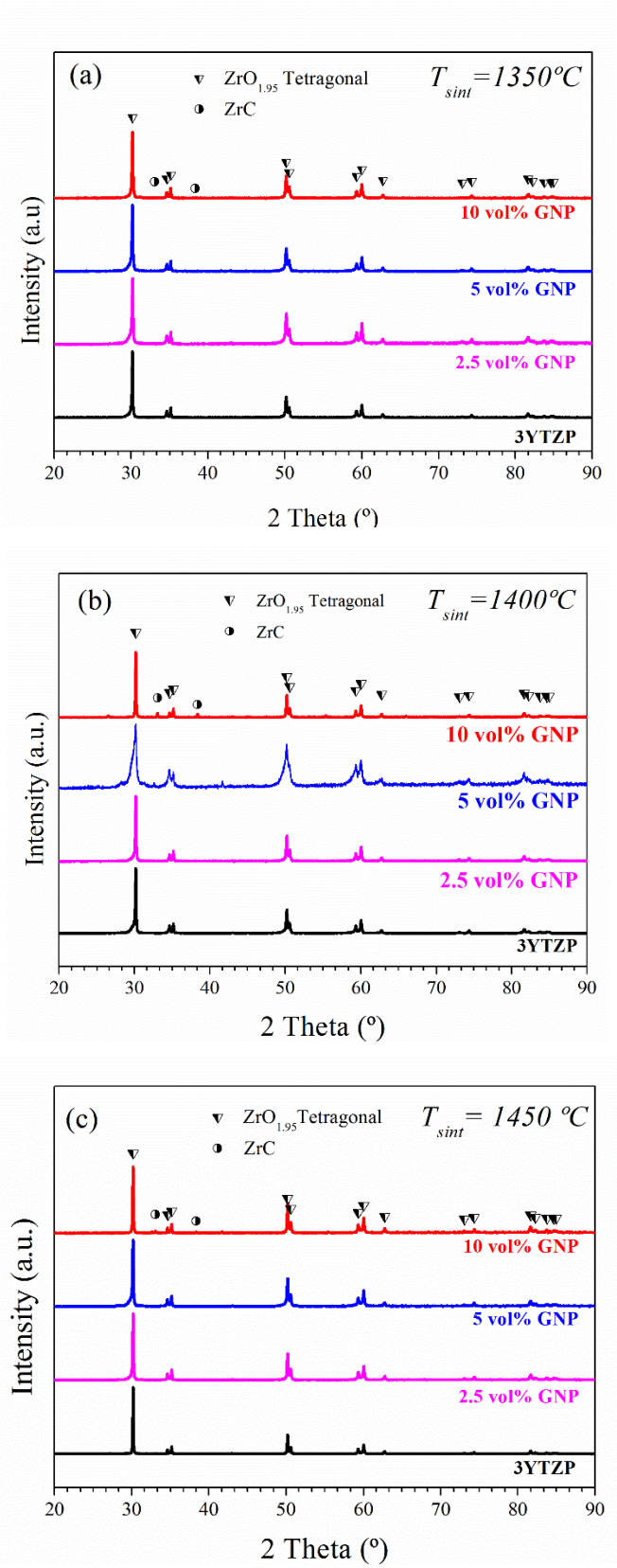

Supplementary figure S1. X-ray diffraction patterns of the GNP/3YTZP composites sintered at (a) 1350 ºC, (b) 1400 ºC and (c) 1450 ºC.

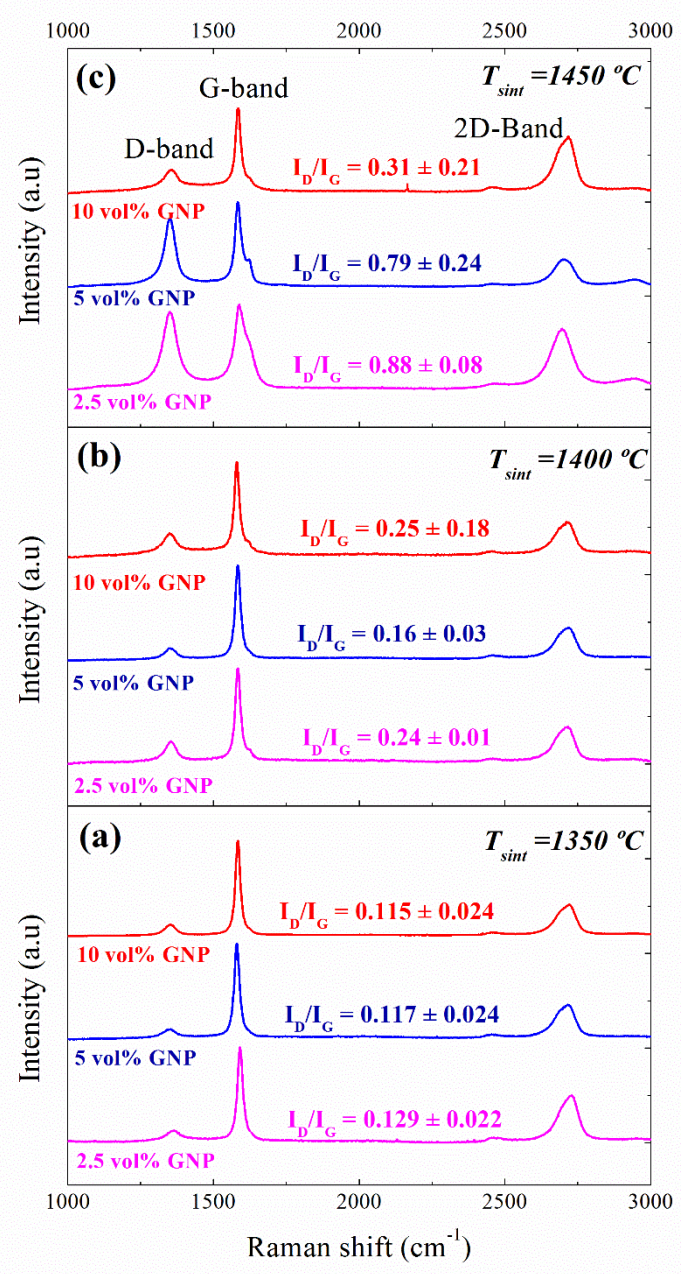

Supplementary figure S2. Raman spectra of the composites with 2.5, 5 and 10 vol% GNP sintered at (a)1350 ºC, (b) 1400 ºC and (c) 1450 ºC.

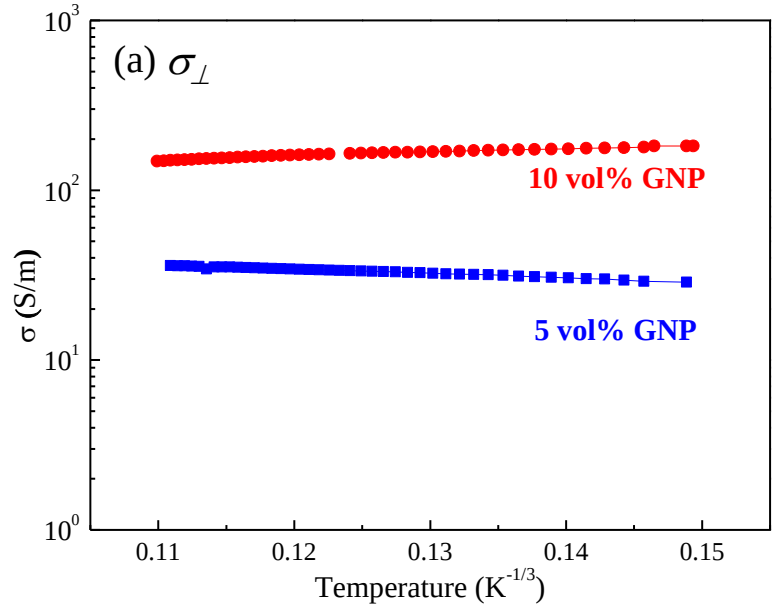

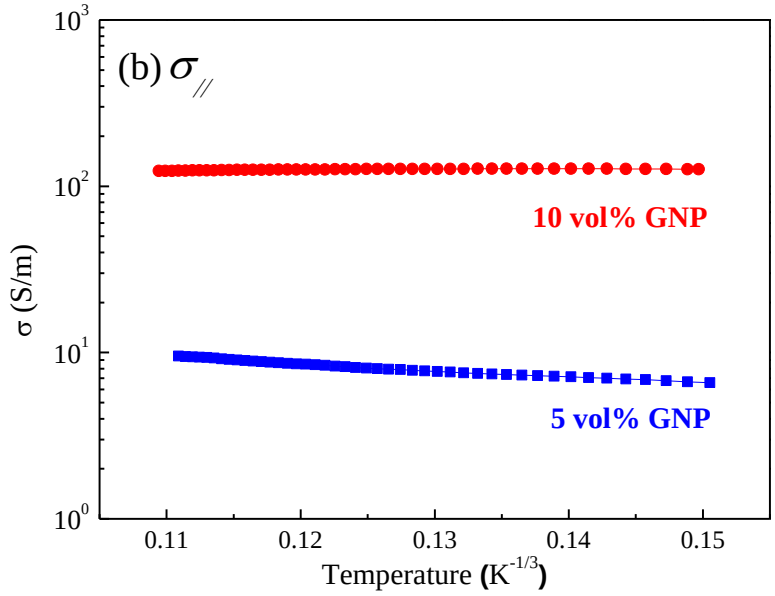

Supplementary figure S3. Electrical conductivity as a function of temperature for the GNP/3YTZP composites sintered at 1350 ºC, plotted according to the 2D-VHR model, (a) $\sigma_{\perp}$ and (b) $\sigma_{//}$.

Table 1. Measured room temperature electrical conductivity and anisotropy factor of the GNP/3YTZP composites

GNP content (vol%)	Sintering temperature (ºC)	$\sigma_{\perp}$ *(S/m)*	$\sigma_{//}$ *(S/m)*	$\sigma_{\perp}/\sigma_{//}$
2.5	1350	(169 ± 7) x10^{-6}	(222 ± 6)x10^{-6}	0.77
5	1350	25.2 ± 1.0	6.66 ± 0.18	3.78 ±0.25
10	1350	177 ± 7	112 ± 3	1.58 ± 0.10
2.5	1400	(39.9 ± 1.6) x10^{-6}	- *	-
5	1400	43.8 ± 1.6	11.9 ± 0.3	3.69 ± 0.23
10	1400	169 ± 6	84.5 ± 2.4	2.00 ± 0.12

*No conductive.

Figure captions

Figure 1: Effect of the GNP content and the sintering temperature on the relative density of the composites.

Figure 2: I_D/I_G ratio from the Raman spectra as a function of the GNP content and sintering temperature.

Figure 3: BSE-SEM images from the cross-section surfaces of the composites sintered at 1350 ºC with (a) 2.5 vol%, (b) 5 vol% and (c) 10 vol% GNP.

Figure 4: HRSEM images of the fracture surfaces of the composites sintered at 1350 ºC with (a) 5 vol% and (b) 10 vol% GNP. The inset shows an area of higher magnification.

Figure 5: (a) Electrical conductivity values reported for GBN/ceramic composites. Values from actual work and reference [14] correspond to $\sigma_{\perp}$.